A THESIS SUBMITTED TO
THE GRADUATE SCHOOL OF NATURAL AND APPLIED SCIENCES
OF ÇANKIRI KARATEKİN UNIVERSITY

DETERMINATION OF NON-ISOTHERMAL REDUCTION KINETICS OF GÖRDES LATERITE ORE-SOMA LIGNITE COAL MIXTURE BY THERMAL GRAVIMETRY

IN PARTIAL FULFILLMENT OF THE REQUIREMENTS
FOR
THE DEGREE OF MASTER OF SCIENCE
IN
CHEMICAL ENGINEERING

BY

AHMED MURES MOHAMMED MOHAMMED

ÇANKIRI

2023

DETERMINATION OF NON-ISOTHERMAL REDUCTION KINETICS OF GÖRDES LATERITE ORE-SOMA LIGNITE COAL MIXTURE BY THERMAL GRAVIMETRY

By Ahmed Mures Mohammed MOHAMMED

June 2023

We certify that we have read this thesis and that in our opinion it is fully adequate, in scope and in quality, as a thesis for the degree of Master of Science.

Advisor **:** Assoc. Prof. Dr. Nesibe DİLMAÇ

Examining Committee Members:

Chairman **:** Assoc. Prof. Dr. Nesibe DİLMAÇ
Chemical Engineering
Çankırı Karatekin University

Member **:** Assoc. Prof. Dr. Mehmet Selçuk MERT
Energy Systems Engineering
Yalova University

Member **:** Assist. Prof. Dr. Semahat DORUK
Chemical Engineering
Çankırı Karatekin University

Approved for the Graduate School of Natural and Applied Sciences

Prof. Dr. Hamit ALYAR
Director of Graduate School

I hereby declare that all information in this document has been obtained and presented in accordance with academic rules and ethical conduct. I also declare that, as required by these rules and conduct, I have fully cited and referenced all material and results that are not original to this work.

Ahmed Mures Mohammed MOHAMMED

ABSTRACT

DETERMINATION OF NON-ISOTHERMAL REDUCTION KINETICS OF GÖRDES LATERITE ORE-SOMA LIGNITE COAL MIXTURE BY THERMAL GRAVIMETRY

Ahmed Mures Mohammed MOHAMMED

Master of Science in Chemical Engineering

Advisor: Assoc. Prof. Dr. Nesibe DİLMAÇ

June 2023

In this study, fine laterite samples from Manisa Gördes mine were calcined, and mixed with dried and fine Soma lignite particles in molar stoichiometric ratio (87% laterite and 13% lignite). Afterwards, the mixtures were heated from ambient temperature to 1000 ºC under N_2 flow at different heating rates; 5, 10, 15, 25, and 40 ºC/min in a thernogravimetric analyser. All experiments were repeated for the same amount of lignite keeping all other parameters the same. Using the weight loss values of both lignite and mixture samples, reduction degrees of the metallic oxides in the ore samples were calculated. Due to the low concentration of the lignite in the mixtures, the highest reduction degree was around 30%. The obtained data was analyzed by non-isothermal kinetic methods and the mean activation energy (E_a) for 0 to 0.18 conversion range of the reduction was determined as 103.44 kJ/mole, 50.32 kj/mole, and 65.68 kJ/mole via Friedman (FR), Flynn-Wall-Ozawa (FWO), and Kissinger-Akahira-Sunose (KAS) methods, respectively. On the other hand, Coats-Redfern (CR) method revealed that the initial stage of the reduction of calcined Gördes laterite by Soma lignite between 0 and 0.3 conversion range progressed under phase boundary chemical reaction control with E_a of 60.01 kJ/mole.

2023, 32 pages

Keywords: Laterite, Lignite, Carbothermic reduction, Non-isothermal reaction kinetics, Thermal gravimetry.

ÖZET

GÖRDES LATERİT CEVHERİ-SOMA LİNYİT KÖMÜRÜ KARIŞIMININ İZOTERMAL OLMAYAN İNDİRGENME KİNETİĞİNİN TERMAL GRAVİMETRİ YOLUYLA BELİRLENMESİ

Ahmed Mures Mohammed MOHAMMED
Kimya Mühendisliği, Yüksek Lisans
Tez Danışmanı: Doç. Dr. Nesibe DİLMAÇ
Haziran 2023

Bu çalışmada, Manisa Gördes madeninden temin edilen, tanecik boyutu 100 μm' den küçük olan ince laterit numuneleri öncelikle kurutulmuş, ardından 900 ºC kül fırınında 18 saat boyunca kalsine edilmiştir. Kalsine cevher numuneleri, kurutulmuş ve yine tanecik boyutu 100 μm' den küçük olan ince Soma linyiti ile molar stokiyometrik oranda (%87 laterit ve %13 linyit) karıştırılmıştır. Karışımlar bir termal gravimetrik analiz cihazında N_2 akışı altında 5, 10, 15, 25 ve 40 ºC/dak. ısıtma hızlarında ortam sıcaklığından 1000 ºC' ye kadar ısıtılarak cevher ve linyit karışımlarının izotermal olmayan indirgenme sürecine ait ağırlık değişimi izlenmiştir. Tüm deneyler, diğer tüm parametreler aynı tutularak aynı miktarda linyit için tekrarlanmış ve linyitin izotermal olmayan şartlardaki ağırlık değişimi de kaydedilmiştir. Hem linyit, hem de karışım numunelerinin ağırlık kaybı değerleri kullanılarak cevher numunelerindeki metalik oksitlerin indirgenme dereceleri hesaplanmıştır. Karışımlardaki linyit konsantrasyonunun düşük olması nedeniyle en yüksek indirgeme derecesi %30 civarında olmuştur. Elde edilen veriler izotermal olmayan kinetik yöntemlerle analiz edilmiş ve indirgemenin 0 ila 0,18 dönüşüm aralığında kalan kısmı için ortalama aktivasyon enerjisi (E_a) Friedman (FR), Flynn-Wall-Ozawa (FWO) ve Kissinger-Akahira-Sunose (KAS) yöntemleri ile sırasıyla 103,44 kJ/mol, 50,32 kj/mol ve 65,68 kJ/mol olarak belirlenmiştir. Coats-Redfern (CR) yöntemi ise, kalsine Gördes lateritinin Soma linyiti ile indirgenmesinin 0 ile 0,3 dönüşüm aralığında kalan ilk aşamasının, "$g(\alpha)=\alpha= k_i.t$" denklemi ile karakterize edilen, faz sınırında kimyasal reaksiyon kontrolü altında ilerlediğini ortaya koymuştur. Özetle, ince kalsine Gördes lateritinin ince Soma

kömürü ile termal analiz cihazında izotermal olmayan indirgenme prosesine ait kinetik triplet (model denklemi, aktivasyon enerjisi ve Arrhenius frekans faktörü) sırasıyla F0, 60,01 kJ/mol, ve 1,44 l^{n-1}. mol $^{1-n}$ $.s^{-1}$ olarak belirlenmiştir.

2023, 32 sayfa

Anahtar Kelimeler: Laterit, Linyit, Karbotermik indirgeme, İzotermal olmayan reaksiyon kinetiği, Termal gravimetri.

PREFACE AND ACKNOWLEDGEMENTS

I would like to express my deepest thanks to my esteemed advisor Associate Professor Dr. Nesibe DİLMAÇ for her great efforts and patience. Also, I would like to thank to Associate Professor Dr. Ömer Faruk DİLMAÇ for his technical assistance. Finally, I would like to thank my beloved family who have been by my side in every moment of my life for their patience, sacrifice and support.

Ahmed Mures Mohammed MOHAMMED

Çankırı-2023

CONTENTS

LIST OF SYMBOLS

α	Reduction degree or reaction extend (-)
A	Arrhenius frequency factor ($l^{n-1}. mol^{1-n}. s^{-1}$)
E_a	Activation energy (kJ/mol)
$f(\alpha)$	Differantial model equation (-)
$g(\alpha)$	Integral model equation (-)
k(T)	Rate constant ($l^{n-1}. mol^{1-n}. s^{-1}$)
R	Universal gas constant (8.314 J/mol.K)
T	Absolute temperature (K)

LIST OF ABBREVIATIONS

CR	Coats-Redfern method
FR	Friedman method
FWO	Flynn-Wall-Ozawa method
HPAL	High pressure acid leaching
KAS	Kissinger-Akahira-Sunose method
RKEF	Rotary kiln electric furnace
TGA	Thermal gravimetric analysis
XRF	X-Ray fluorescence

LIST OF FIGURES

LIST OF TABLES

1 INTRODUCTION

1.1 Nickel

Today, nickel is widely employed in a wide range of products, including alloying components for steelmaking, chemicals, aerospace industires, magnets, and rechargeable batteries.

To date, conventional nickel production from sulfide type nickel ores through pyrometallurgical processes has been used to supply nickel products for the metal market. However, as sulfide nickel production declines, nickel extraction from oxide ores (laterites) is becoming more popular. Additionally, almost 80% of known nickel reserves and significantly higher cobalt reserves are found in lateritic type nickel deposits (Halikia *et al*. 2002). As a result, laterites will become more important in the nickel production process in the future.

Pyrometallurgical and hydrometallurgical processes can both be used to recover nickel from lateritic ores. Drying, calcination/reduction, and electric furnace smelting are common steps in the standard flowsheet used by the majority of pyrometallurgical processes (ferronickel and matte smelting). The Caron process and high pressure acid leaching (HPAL) are the two most popular hydrometallurgical procedures.

When a metal is alloyed, nickel increases its strength, hardness, and corrosion resistance. The nickeliferous alloys used in stainless steel and the copper nickel alloys used in coinage metal are the most well-known.

Both nickel ores of the sulfide and laterite types can be found in Turkey. Sulfide type ores are primarily found in Bursa and Bitlis, while laterite type ores are mostly found in Manisa's Çaldağ and Gördes regions (Warner *et al.* 2006). Although new nickel deposits have been found at Mihaliççik (Eskişehir), Banaz (Uşak), and Divriği (Sivas),

adequate information regarding the reserves of the deposits could not be collected due to incomplete reserve studies. Table 1.1 lists Turkey's nickel ore reserves.

Table 1.1 Nickel ore reserves of Turkey

Region	Probable Reserve	Possible Reserve
Manisa- Çaldağ	37,900,000	-
Manisa-Gördes	68,500,000	-
Bursa- Yapköy	82,000	81,000
Bitlis-Pancarlı	-	15,500

Nickel is primarily consumed by the steelmaking industry. More than 60% of the world's nickel production is used in stainless steel production to improve corrosion resistance and strength. Nickel alloy production ranks second in terms of nickel usage. Because of their high temperature resistance and fracture toughness, nickel alloys are used in a wide variety of applications. Nickel's other major applications include ferrous metallurgy, coinage, and plating. Graphical representation of nickel usage by use is given in Figure 1.1.

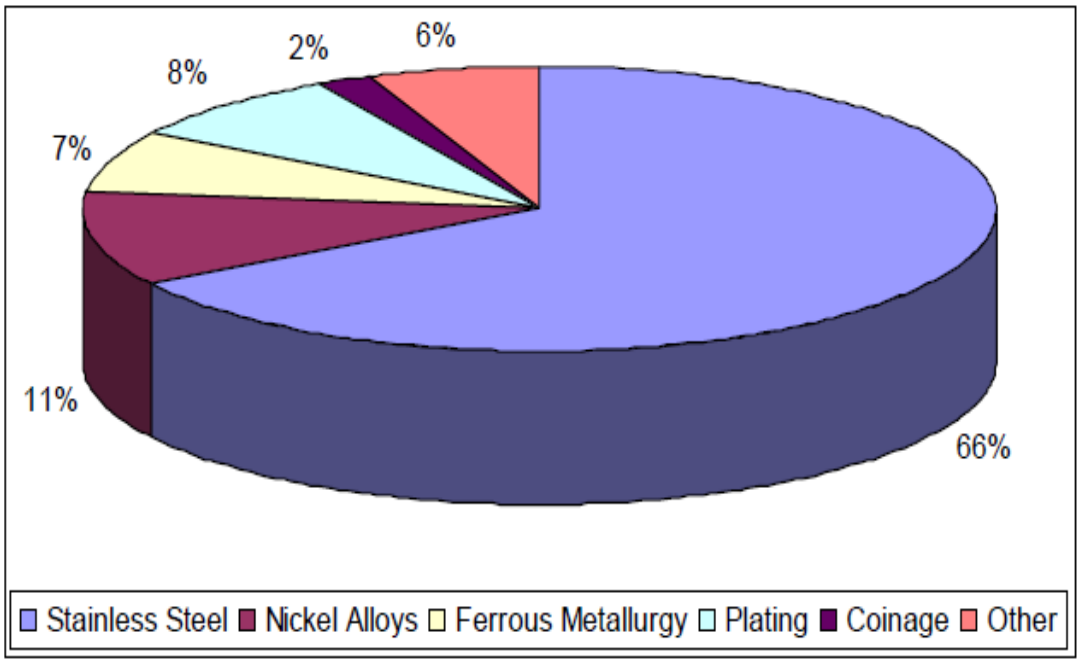

Figure 1.1 Nickel consumption by use (Thorne *et al*. 2009)

However, due to current high nickel prices, treating low grade nickel ores is profitable this will pave the way for future projects that will contribute to annual nickel production as shown in the supply vs. consumption diagram in Figure 1.2.

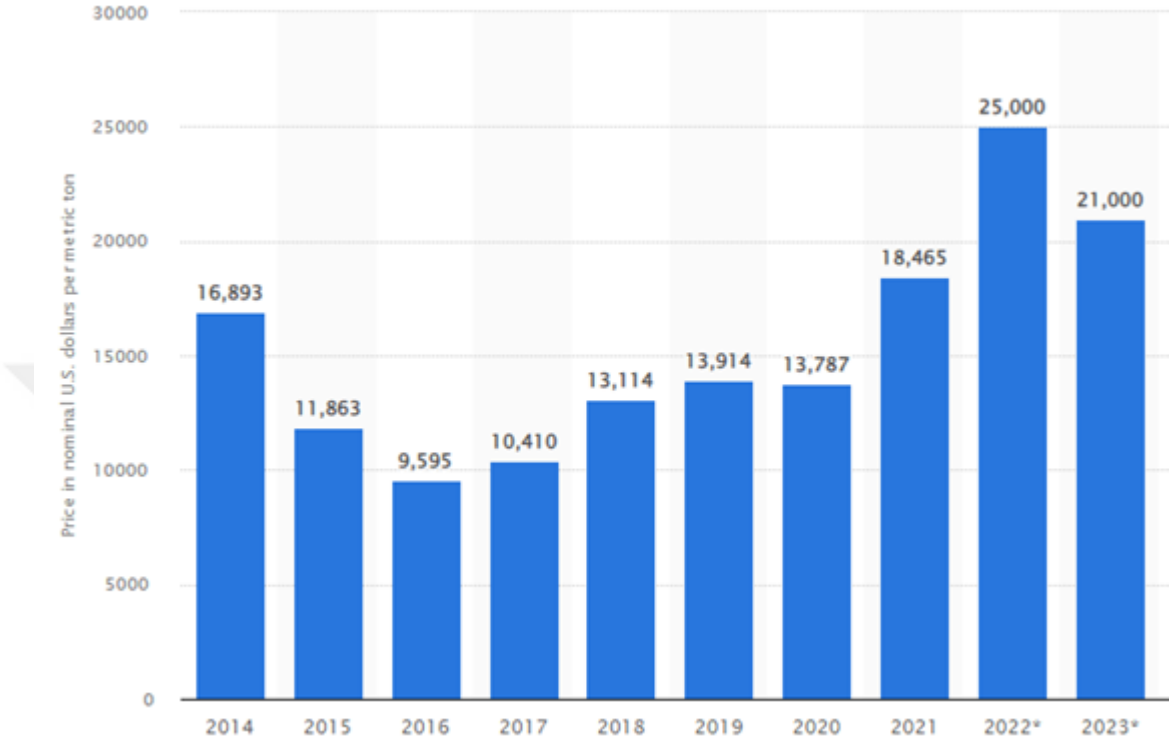

Figure 1.2 Nickel prices between 2014-2023

1.2 Characteristics

The physical specifications of nickel metal are summarized as follows: - It is a silvery-white lustrous metal, belonging to the group of IVB transition metals, a relatively low conductor of electricity and heat, and it is alloyed with other metals to increase its strength and resistance to corrosion. Nickel is widely used in stainless steel, magnets, electroplating and other fields. About 65% of nickel is consumed in the manufacture of stainless steel and heat-resistant steel for the construction, military, marine, transportation and aerospace industries. So the demand for it is great, and it is constantly growing.

1.3 Nickel Production Processes

The kind and mineralogy of the lateritic ore affect the method of nickel extraction. This ore's complicated mineralogy has given rise to numerous pyro and hydrometallurgical extraction methods, four of which are commercially viable: matte smelting, ferronickel smelting via the rotary kiln-electric furnace (RKEF) process, high pressure acid leaching (HPAL), and the Caron method (Dalvi *et al.* 2004).

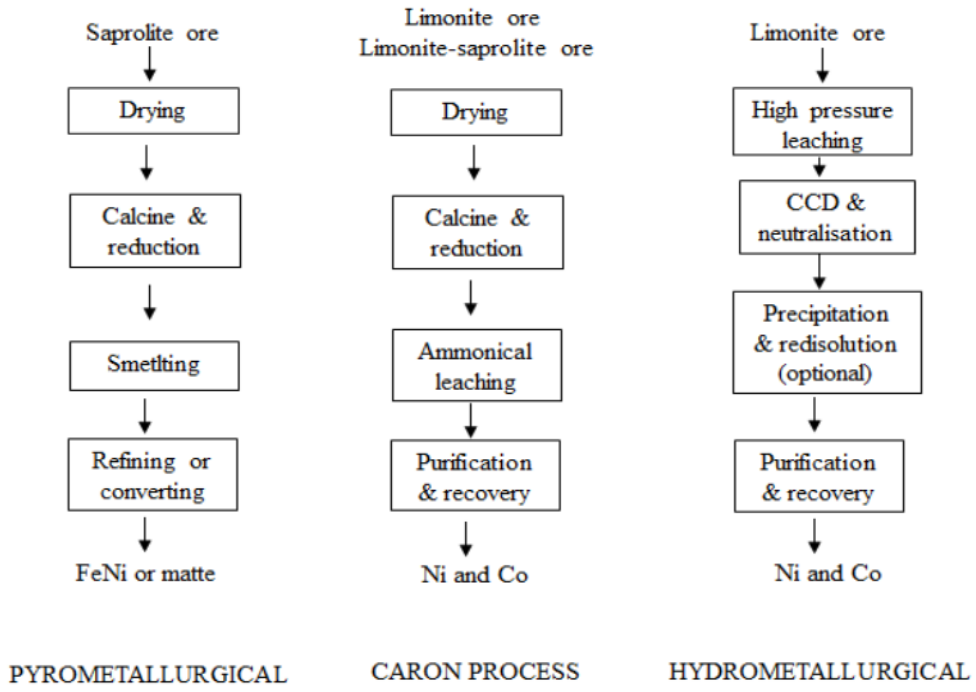

Figure 1.3 Flow chart for various methods of processing laterites (Bunjaku *et al*. 2010)

HPAL and the Caron process are the two most often used hydrometallurgical processes for treating laterites. Although the Caron process is a hybrid of pyro and hydro techniques, it is most commonly classified as a hydrometallurgical process (Figure 1.3).

Limonitic ore is leached in sulfuric acid using the HPAL process, which employs high temperatures (245-270°C) and pressures (up to 5,4 MPs). Through the process of Counter-Current Decantation, a solid residue is removed from the liquid solution. The solution can be purified in a variety of methods. All of these products may be used to

make nickel oxide, briquettes, and electrolytic nickel. Intermediate products such as mixed hydroxides and mixed sulfide are produced by some plants. The ore to be processed with HPAL must include as little saprolite as feasible since nickel extraction from silicate structures is more difficult (Rhamdhani *et al*. 2009).

The Caron process is the oldest method for treating limonite ores of low grade. It consists of drying, reduction roasting, and leaching in a buffered ammoniacal solution. The nickel and cobalt oxides and some iron oxide (Dalvi *et al.* 2004) in the ore are selectively reduced to create alloy (metallic) particles during roasting at about 700°C. An ammonium carbonate solution is subsequently used to leach these particles away (King 2005).

Nickel carbonate is produced when the leached fluid has been purified to a high degree. Using a reducing gas, a solid intermediate product is reduced to nickel metal. An excellent source of iron is the leaching residue (Purwanto *et al.* 2003). Limonitic and saprolite ores may be processed using the Caron process, however the recovery rate drops down as the fraction of saprolite ores rises. At the temperatures utilized in this method, nickel and cobalt in the silicate matrix are difficult to decrease (Dalvi *et al.* 2004).

Historically, saprolite ores were processed using smelting techniques. By adding sulfur, pyro techniques include smelting to a Ni-Fe-S matte and smelting to ferronickel. Due to nickel's substantially lower free energy, its separation from gangue components such as silica is rather straightforward. Allows for the complete reduction of nickel oxide while limiting the amount of iron oxide being reduced. However, selective reduction cannot be used to completely separate nickel from iron (Diaz *et al*. 2008).

The technique is based on the fact that nickel has a higher affinity for sulfur than iron and that iron has a higher affinity for oxygen than nickel. A flux, a reductant, and a sulfur source are added to the ore. A sulfide mineral or elemental sulfur can be used as a sulfur source. Almost all of the nickel and a significant portion of the iron are reduced and forms a matte when it reacts with sulfur (Canterford 1975).

The ore is smelted in RKEF process to produce a ferronickel product. The RKEF process consists of two stages: drying, calcination, and partial reduction of the ore in a rotary kiln, followed by smelting in an electric arc furnace. The ferronickel product may include, depending on the ore grad (20-40%) nickel (Canterford 1975).

1.4 Thermal Gravimetric Analysis (TGA)

Thermal Gravimetric Analysis (TGA) is a type of thermal analysis in which the mass of a sample is measured over time as the temperature changes. This measurement tells us about physical and chemical processes, like phase changes, absorption, adsorption, and desorption. It also tells us about chemisorption's, thermal decomposition, and solid-gas reactions (e.g., oxidation or reduction).

A thermo gravimetric analyzer is used to perform a TGA, which is a type of thermo graphic analysis. As the temperature of a sample changes, a thermo gravimetric analyzer measures the sample's mass. Thermo gravimetric analysis relies on the three basic measurements of mass, temperature, and time to obtain a wide range of additional measurements.

A typical thermo gravimetric analyzer comprises of a precision balance and sample pan housed within a furnace with programmable temperature control. To induce a thermal reaction, the temperature is normally increased at a consistent pace (or in some applications, the temperature is regulated for a constant mass loss). The thermal reaction may occur in a variety of atmospheres and pressures, such as ambient air, vacuum, inert gas, oxidizing/reducing gases, corrosive gases, larborizing gases, liquid vapors, or "self-generated atmosphere"; as well as a high vacuum, high pressure, constant pressure, or a controlled pressure.

The thermo gravimetric data acquired from a thermal reaction is shown as mass or percentage of starting mass on the y axis vs. either temperature or time on the x axis. This graph, which is frequently smoothed, is known as a TGA curve.

1.5 Non-Isothermal Reaction Kinetics

Laterite is composed of a group of metal oxides such as nickel and iron oxide. The nickel oxide contained in the limonitic ore exists in a solid solution with goethite.

Eq. (1.1) may be used to calculate the laterite ore conversion or reduction degree (α). "m(t)" is the weight of the ore sample at any point in the run, "mo" is the weight of the sample in its oxidized state, and "mr" is the weight of the sample in case of full reduction (Lv *et al.* 2017).

$$\alpha = \frac{mo-m(t)}{mo-mr} \tag{1.1}$$

The rate of a solid-state reaction (dα/dt) can be described by the well-known kinetic law given in Eq. (1.2).

$$\frac{d\alpha}{dt} = k(T).f(\alpha).\ c^n \tag{1.2}$$

where "α" is the conversion degree of the solid reactant, "f(α)" is the differential model function describing the mechanism, and "k(T)" is the temperature-dependent reaction rate constant (Fedunik-Hofman *et al.* 2019). In this equation, k(T); the temperature dependent reaction rate constant, f(α); differential model function describing the reaction mechanism, C; concentration of reactant and n; shows the order of the reactions.

If Equation (1.2) is rearranged and integrated, Equation (1.3) is obtained.

$$g(\alpha)= \int \frac{d\alpha}{f(\alpha)} = \int k(T).c^n.dt \tag{1.3}$$

g(α) appearing in this equation is the integral model function describing the reaction mechanism. Since k(T) has a constant value for experiments performed under isothermal conditions, the analytical solution of the above equation can be done easily.

For this purpose, if the expression "k(T).C^n" is redefined as in Eq.(1.4) and combined by substituting it into Eq. (1.3), Eq. (1.5) is obtained.

$$ki=k(T).\ c^n \quad (1.4)$$

$$(\alpha)= k(i).\ t \quad (1.5)$$

Equation (1.5) is a very useful equation for explaining the reaction mechanism. Specifically, the equation representing the "t-g(α)" data for the interaction with the highest linear regression coefficient (R^2) among the different g(α) functions shown in Table 1.2 is the integral model function of the interaction. The slope of the resulting line is the 'ki' value of the reaction for the temperature and concentration at which the experiments are performed.

Table 1.2 Most common f(α) and g(α) for gas-solid reactions (Vyazovkin 1999)

Reaction Model	**Symbol**	**f(α)=(1/Ki).(dα/dt)**	**g(α)=ki.t**
One-dimensional diffusion model	D1(α)	1/(2α)	α 2
Two-dimensional diffusion model	D2(α)	(-ln(1-α)) -1	(1-α)ln(1-α)+ α
Three-dimensional diffusion model (Jander equation)	D3(α)	(3/2)(1-α)2/3(1-(1-α)1/3)	(1-(1-α)1/3)2
Three-dimensional diffusion model (Ginstein-Brounshtein equation)	D4(α)	(3/2)((1-α)-1/3-1)	(1-2α /3)-(1-α)2/3
Chemical reaction controlled model (infinite plate)	F0(α)	1	α
random nucleation model	F1(α)	1-α	-ln(1-α)
Chemical reaction controlled model (shrinking cylinder)	R2(α)	2(1-α)1/2	1-(1-α)1/2
Chemical reaction controlled model (shrinking sphere)	R3(α)	3(1-α)2/3	1-(1-α)1/3
Two-dimensional kernel growth model (Avrami-Erofe'ev equation) (m=2)	A2(α)	2(1-α)(-ln(1-α))1/2	(-ln(1-α)) 1/2
Three-dimensional kernel growth model (Avrami-Erofeev equation) (m=3)	A3(α)	3(1-α)(-ln(1-α))2/3	(-ln(1-α)) 1/3

1.5.1 The Friedman (FR) method

$$\frac{d\alpha}{dt} = A.e^{\left(-E_a/R.T\right)}.f(\alpha) \quad (1.6)$$

By taking the natural logarithm of each side of Equation (1.6) the model-free (isoconversional) Friedman's equation (FR) given in Equation (1.7) is obtained.

$$\frac{d\alpha}{dt} = \left(\frac{-Ea}{R.T}\right) + \ln\left(A.f(\alpha)\right) \quad (1.7)$$

By inserting the linear heating rate ($\beta = \frac{dT}{dt}$) into the left-hand side of Eq. (1.7), Eq. (1.8) is obtained (Wang 2019).

$$\ln\left(\beta.\frac{d\alpha}{dT}\right) = \left(\frac{-Ea}{RT}\right) + \ln\left(A.f(\alpha)\right) \quad (1.8)$$

In this context, if both sides of Equation (1.7) are divided by "β" and rearranged, we can obtain "Ea" for a particular "α" without making any assumption on the reaction model from the negative slope of the straight line showing the variation of "ln[β ($\frac{d\alpha}{dT}$)]" against "1/T" for different heating rates.

1.5.2 Flynn-Wall-Ozawa (FWO) method

In integral model-free Flynn-Wall-Ozawa (FWO) method which employs Doyle's approximation for the solution of "g(α)", linear fitting of "ln(β)" versus "1/T" couples obtained at different heating rates for a particular conversion (α) gives a straight line with a slope of "-1.051 Ea/R" (Wang 2019) as seen on Eq. (1.9).

$$ln(\beta) = ln\left(\frac{A.Ea}{R.g(\alpha)}\right) - 5.331 - 1.051\,\frac{Ea}{R.T} \quad (1.9)$$

1.5.3 Kissinger-Akahira-Sunose (KAS) method

In integral model-free Kissinger-Akahira-Sunose (KAS) method which utilizes Murray and White approximation for the solution of "g(α)", one can calculate "Ea" from the slope of the straight line by plotting "ln(β/T^2)" versus "1/T" couples obtained at different heating rates for a particular "α" (Bartocci *et.al.* 2019) as seen in Equation (1.10).

$$(\frac{\beta}{T2})=ln(\frac{A.R}{g(\alpha).Ea})-\frac{Ea}{R.T} \quad (1.10)$$

1.5.4 The Coats-Redfern (CR) method

The Coats-Redfern equation has been extended to evaluate other kinetic parameters such as the degree of interaction and the exponential factor (Bunjaku *et al.* 2012). Where the equation refers to the relationship between the degree of transformation and the change in temperature, as given in Equation (1.11).

$$\ln\frac{AR}{\beta E}(1-\frac{2RT}{E})-\frac{E}{2.3\,RT} = \mathrm{Ln}\,(\frac{1-(1-\alpha)\^(1-n)}{T\^2(1-n)}) \quad (1.11)$$

1.6 Aim of the Study

The importance of this study lies in the search for the possibility of reducing nickel and iron oxides in the laterite Gordes ore using Soma lignite coal. Laterite ore is available in Turkey in large quantities. Turkey is the eighth steel producer in the world. Coal is also available in Turkey in large quantities. Therefore, the process of extracting minerals from laterite ore is of great importance, as these minerals contribute to the development of the industrial economy in Turkey, and provide for the industrial needs these minerals.

The aim of this study was to extract nickel from lateritic ores obtained in Turkey's Gördes (Manisa) region. Extracting these traditional minerals from laterite ore requires

high energy, with environmental pollution, by emitting polluting gases into the atmosphere at a high cost.

The current study examines the possibility of reduction of minerals iron and nickel under certain conditions with less energy and the emission of polluting gases in smaller quantities. And the economic cost of this process is lower compared to traditional methods.

2 LITERATURE SUMMARY

The process of literate reduction is one of the important processes in metallurgy, and many researches have been conducted in this direction. Laterites require using traditional separation methods. Thus, efficient processing and utilization of laterite ores is a matter very important.

Back in the twenties of the last century, there was a great diversity between the kinetic model and activation energy values, especially in studies aimed at determining reduction kinetics. There is a wide range of experimental parameters such as file configuration reducing the gases used in experiments and the chemical and physical properties of the ores, particle sizes, working temperature, and types of reactors were used effectively in the emergence of this condition. For all these reasons, the literature about the study presented is very extensive, and in this section, especially coal carbon dioxide and H_2. The results of a relatively recent study using gases and coal will be included (Conard *et al.* 1978). Temperatures between 350 and 850°C, the nature of the reducing environment, and the ratio of oxide to reductant were all examined. The reducing potential determined both the nickel metallization and the nickel grade in the final ferronickel alloy. The nickel grade rose with the water concentration of the initial reducing environment while reducing hydrogen. Additionally, when the water content grew, nickel metallization reduced as more nickel reported to the spinel phase, whereas wustite predominated under more reducing circumstances. The bulk of the nickel reported to the alloy if pure hydrogen or carbon monoxide was utilized. As a result, it would be most effective to operate near the stoichiometric need for the reduction of all nickel oxide.

Canterford and Turnbull (1980) found that carbon monoxide had better selectivity than hydrogen at lower temperatures (650°C), resulting in a ferronickel with a much higher nickel grade. Both reducing gases reacted identically at temperatures over 650°C, owing to the full reduction of all iron and nickel oxides in the ore. The behavior of an equimolar mixture of the two reducing gases was intermediate below 650°C and identical to the pure gases above this temperature. A stoichiometric surplus of hydrogen

was present at all temperatures examined, allowing for a highly high (>90%) conversion of nickel oxide to nickel metal. Carbon monoxide atmospheres could not accomplish the same conversion without significantly increasing the temperature or the reduction potential of the atmosphere. Ferronickel and nickel metallization grades are strongly influenced by all three factors. Temperatures beyond 600°C were recommended to produce high reaction rates, even though nickel metallization could be performed below 600°C.

Utigard and Bergman (1992) analyzed the reduction of a saprolitic ore by a combination of H_2 and CO_2. According to their model, at an H_2: CO ratio of 1,6 and a temperature of 600°C, no metallic iron should occur and nickel metallization should reach around 50%, but at the same gas ratio and a temperature of 1000°C, nickel metallization should reach almost 90%. The scientists also noticed that no metallic iron should occur at a gas-to-iron ratio of less than 1.6, and that a greater gas-to-iron ratio enhanced the pace and extent of metallization. Lower temperatures and reductant gas ratios should encourage more selectivity of the nickel oxide over the iron oxide, resulting in higher quality ferronickel, according to these findings, which are in general agreement with those of the conclusion that a pure nickel metal product may be generated under specified conditions, on the other hand, directly contradicts Canterford and Turnbull's findings (Canterford and Turnbull 1980).,

The thermo-gravimetric analysis (TGA) method was used to evaluate the reduction of nickel laterite ore with carbon monoxide to create Fe-Ni alloy by Li *et al.* (2018). Researchers used non-isothermal reduction assays to measure the distinct phases of reduction and reaction products in each condition, heating at a constant rate of 10 °C/min from room temperature to 1200 °C. Through the use of X-ray diffraction analysis and the combination of mass loss measurements with theoretically derived values, the products of several reduction steps were identified and a reaction route was formed. The temperature dependency of the reduction kinetics was evaluated using isothermal reduction experiments at temperatures ranging from 500 °C to 1100 °C. The rate-controlling step in the isothermal testing was further determined by fitting several kinetic models to the experimental data. The rate of CO flow and the mass of the sample

were then studied in two sets of TG experiments. From 500 °C to 1100 °C, the decrease rate was shown to rise by an order of magnitude. Reduction temperatures from 700 °C to 1100 °C result in the formation of more alloy products and an increase in the apparent activation energies from 8.6 to 14.7 kJ/mol. As a result, it was hypothesized that the rate-limiting processes are CO diffusion in the bulk gas and via the pores of the laterite ore sample bed.

Under an argon environment, the non-isothermal reduction kinetics of nickel laterite with graphite was studied by Lv *et al.* (2018). The reduction of nickel laterite was conducted at various heating speeds (10, 15, and 20 K/min), and the evolved gas was measured in real time using a mass spectrometer. The activation energies were calculated using the Kissinger-Akahira-Sunose (KAS) method and the reaction kinetics were calculated using the model-fitting (Coats-Redfern) technique. According to the results, the reduction process may be classified into three stages based on the degree of conversion 0–0.45, 0.45–0.75, and 0.75–1.0, respectively. In the first stage, the average activation energy was 351.03 kJ/mol, and the kinetic model was consistent with the two-dimensional diffusion function. In the second step, the model of three-dimensional diffusion function was calculated as the kinetic function, and the average activation energy was determined to be 322.89 kJ/mol. The average activation energy in the third stage was 341.45 kJ/mol, and the kinetic model was consistent with the chemical reaction function.

To extract ferronickel from low-grade nickel laterite ore, a coal-based direct reduction technique was adopted by Zhang *et al.* (2020). The impacts of basicity on the compressive strength, metallization rate, microstructure, and reduction properties of nickel-bearing laterite ore pellets were examined. Iron metallization and pellet compressive strength increase with increasing basicity, according to the study's findings. The rotary kiln's ideal reduction temperature should be between 1150°C and 1250°C with a pellet basicity of 0.56 to avoid the formation of rings. Under optimal process conditions, metallized pellets are composed mostly of ferronickel ([Fe, Ni]), forsterite, ferroan, and pigeonite.

As the costs involved with extracting nickel from sulphide ores climb, nickeliferous limonitic laterite ores are becoming an increasingly appealing source of metallic nickel. In contrast to sulphide ores, laterite ores cannot be concentrated using standard mineral processing processes like as froth flotation. The pyrometallurgical solid-state reduction of nickeliferous limonite ores at relatively low temperatures, followed by magnetic separation, would be a possible concentration technique. In a study by Elliott *et al.* (2015), a thermodynamic model was created to evaluate the reduction of a nickeliferous limonitic laterite by hydrogen using a variety of reductants. At temperatures of 673–873 K, nickel recovery to the ferronickel phase was projected to be more than 95%. High recoveries over a broader temperature range were achieved with reductive additions above the stoichiometric need, although the nickel quality of the ferronickel reduced.

The production of ferronickel from nickel laterite ore requires a lot of energy, especially when the ore has a low nickel concentration. Before smelting, selective reduction–beneficiation of laterite ore to obtain high nickel content nickeliferous concentrate and forsake gangue minerals might be used as a pre-treatment. Zhua *et al.* (2012) used a combination of 6 percent calcium sulfate and 5 percent reductant coal to selectively reduce nickel laterite ores at 1100 °C for 60 minutes. Wet magnetic separation was used to separate the reduced ore. Experiments reveal that a high nickel content nickeliferous concentrate comprising 6.0 percent Ni and a nickel recovery of 92.1 percent may be obtained with almost 75% of the reduced ore containing low nickel concentration being discarded. The results of the experiments revealed that reduction selectivity is mostly influenced by the reduction environment and silica concentration. Nickel oxide had been decreased, and nickel had mostly enriched into a Fe–Ni phase, according to the microscopic analysis. Sulfur increased Fe–Ni particle development from 5.8 m to 16.1 m and improved Ni enrichment in metallic phases when sulfur was present.

There is interest in developing novel procedures to extract nickel from oxides nickeliferous laterite deposits as worldwide nickel sulphide resources become harder to access. Due to their complicated mineralogy, nickel laterites are not susceptible to considerable upgrading, unlike sulphide ores. In a work by Marzoughi *et al.* (2020), firstly standard procedures used to handle nickeliferous limonitic laterites and recent

research in the field. A thermodynamic model is constructed to simulate the roasting process and help determine process parameters to optimize nickel recovery and grade and reduce magnetite concentration in the concentrate. A two-stage procedure including reduction roasting and thermal growth in a tube furnace or rotary kiln furnace, followed by magnetic separation, was also studied. Thermo gravimetric, differential thermal, and mineral liberation analyses were used. The nickel grades and recovery results were compared to published data.

In a study by Jankovic *et al.* (2008), the nickel oxide powder samples were made using the sol–gel method. Temperature-programmed reduction (TPR) was used to explore the non-isothermal reduction of nickel oxide using hydrogen at four distinct heating rates (2.5, 5, 10, and 20 C/min^{-1}). Stationary point (SP), Kissinger, Friedman, Flynn–Wall–Ozawa, and Kissinger–Akahira–Sunose techniques were used to calculate reaction kinetics parameters (Ea, lnA). The Malek's kinetic approach was used to choose the best appropriate kinetic model and calculate a full set of kinetic parameters. The examined reduction process' kinetic model was established, and this model correlates to the empirical two-parameter Sesták–Berggren equation, which provides a more quantitative explanation. Ea=90.8kJmol-1; lnA=19.50, ($f(\alpha)=\alpha 0.63(1-\alpha)1.39$) are the kinetic triplets found for the examined process. By comparing computed and experimental non-isothermal data, the trustworthiness of kinetics parameters estimated from TPR data is verified. The kinetic triplet's consistency was determined by comparing experimental and computed rate curves at a constant heating rate. The mechanism of nickel oxide reduction by hydrogen was considered in accordance with the observed data.

3. MATERIAL AND METHOD

3.1 Laterite Ore and Soma Lignite

The laterite ore samples used in this study were supplied from Gördes (Manisa, Türkiye) mine via Meta Nickel Cobalt Company (META NİKEL KOBALT A.Ş.). The coarse ore pieces were crushed in a jaw breaker and sieved using standard sieves. Fine ore fractions with diameters smaller than 100 μm were used in experiments. The ore samples were calcined at 900 ºC for 18 hours in a muffle furnace to obtain more durable and mechanically resistant particles. The XRF chemical composition of the raw laterite ore is given in Table 3.1. It is essential to underline that Fe_2O_3 and NiO composition of the calcined ore increased up to 46.50% and 3.51% respectively due to the losses during calcination.

Table 3.1 Chemical composition of Gördes laterite ore

Fe_2O_3	Al_2O_3	SiO_2	NiO	CaO	Cr_2O_3	MgO	SO_3	Other
42.31	8.82	33.11	3.19	3.66	1.67	2.22	0.5	4.52

The lignite samples were supplied from Soma mines via General Directorate of Turkish Coal Enterprices (Türkiye Kömür İşletmeleri Kurumu A.Ş). After drying, crushing and sieving procedure, fine lignite fractions smaller than 100 μm were reserved for the experiments. The approximate and ultimate analysis of the dried Soma lignite is given in Table 3.2.

Table 3.2 Proximate and ultimate analysis of Soma lignite

Proximate Analysis (% w/w, Dry basis)	**Volatile**	**Fixed Carbon**	**Moisture**	**Ash**	**Lower heating value (MJ/kg)**
	42.08	43.76	0	14.16	24.91

Ultimate Analysis % w/w, Dry basis	**C**	**H**	**N**	**S**	**O**	**Ash**
	66.53	4.63	1.27	1.11	11.56	14.16

3.2 Experimental Set-up

The carbothermic reduction experiments within the scope of this study were carried out in the thermogravimetric analyzer (TA Instruments SDT Q600) shown in Figure 3.1.

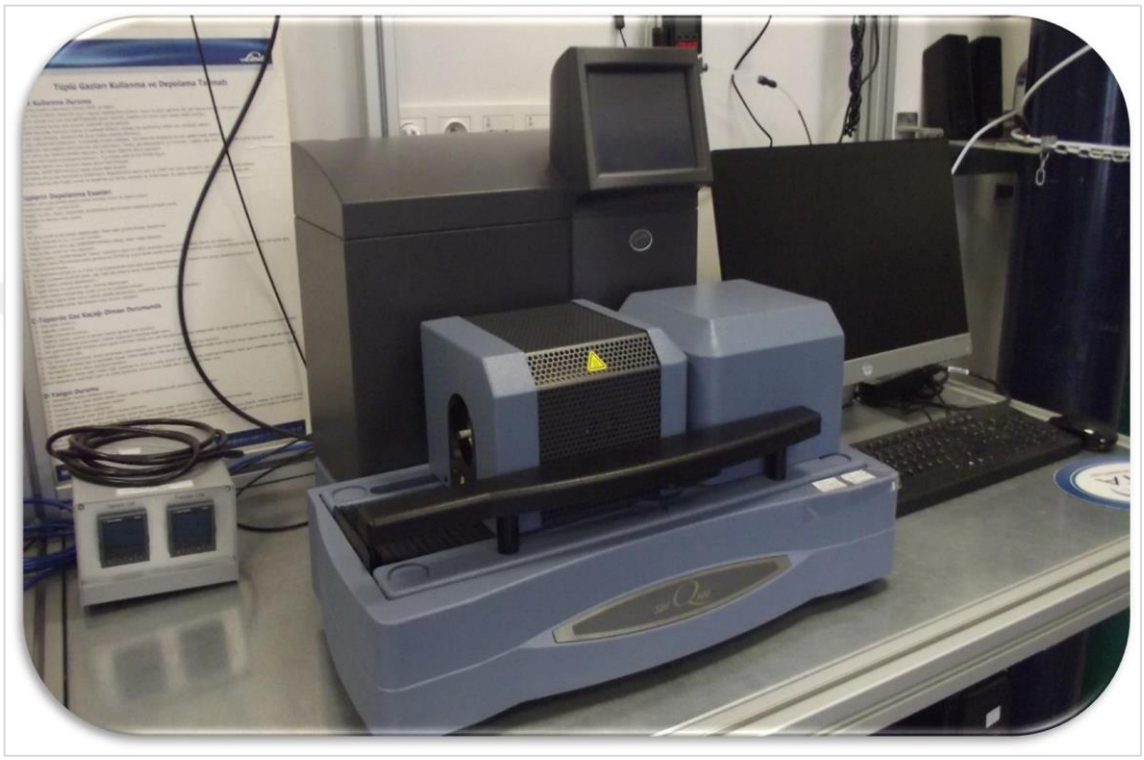

Figure 3.1 Experimental set-up

The calcined ore and lignite samples were mixed in a stoichiometric ratio (87% calcined ore and 13% dried lignite by mass) considering the minimum reductant requirement for the complete reduction of the iron and nickel oxides in the ore into their metallic forms. After obtaining a homogenous mixture, approximately 30 mg of sample was placed into an alumina crucible and heated in the TGA analyzer from ambient temperature to 1000 ºC under 20 ml/min. of N_2 flow. The experiments were performed at 5 different heating rates; 5, 10, 15, 25, and 40 ºC/min. All experiments were repeated for the same amount of lignite keeping all other parameters the same. Since the laterite was calcined in the muffle furnace prior to the experiments, no discernible weight loss was observed in the

thermogram of the ore sample. That is why the experimental procedure included solely lignite and "lignite-laterite" mixtures.

3.3 Method

The reduction degree of the metallic oxides in the laterite ore was calculated according to the method described by Ubando *et al.* (2019). In this method, an imaginary TGA curve ($TGA_{theroretical}$) is created considering how the weight of the mixture would change with increasing temperature, in case there was no reaction between the ore and the lignite according to the Equation (3.1), where "TGA" and "y" correspond to the TGA curve and weight fraction, whilst the subscripts "L" and "S" demonstrate calcined laterite ore and Soma lignite, respectively.

$$TGA_{theoretical} = (TGA_L \times y_L) + (T_S \times y_S) \quad (3.1)$$

Afterwards, the difference between the theoretical curve and the real one ($TGA_{experimental}$) was calculated using Microsoft Excel. Since "$TGA_{experimental}$" includes both the effects of volatilization of the lignite and the reduction of the metal oxides, however "$TGA_{theroretical}$" includes solely the decreases caused by volatilization of the lignite, the gap between "$TGA_{theroretical}$" and "$TGA_{experimental}$" provides a measure for determination of the reduction degree as seen in Equation (3.2).

$$Reduction\ Degree\ (\%) = \frac{TGA_{theoretical} - TGA_{experimental}}{w_O} \times 100 \quad (3.2)$$

"w_O" seen in Equation (3.2) is the weight of the oxygen bounded to the metallic oxides in the calcined laterite sample.

4. RESULTS AND DISCUSSION

4.1 Thermograms

The weight loss curves of Soma lignite, and "lignite-laterite" mixtures obtained at different heating rates are given in Figure 4.1, Figure 4.2, Figure 4.3, Figure 4.4, and Figure 4.5, respectively. Owing to be calcinated before the experiments, practically no change was observed in the weight of the laterite samples during heating up to 1000 ºC under N_2 atmosphere. Thus, solely the the weight changes of lignite, and "lignite-laterite" mixtures were examined in the following sections.

As seen from Figure 4.1, Figure 4.2, Figure 4.3, Figure 4.4, and Figure 4.5, the lignite samples underwent approximately 42% weight loss at all heating rates which is in accordance with the volatile matter percent given in Table 3.2. On the other hand, the weight loss of "lignite-laterite" mixtures eventuated between 5.46% and 7.85% depending on the heating rate. Those losses emerged from both volatilization of the lignite, and as well, from the carbothermic reduction of the ore *i.e.* the removal of the oxygen from metallic oxides in the laterite as a result of interacting with lignite.

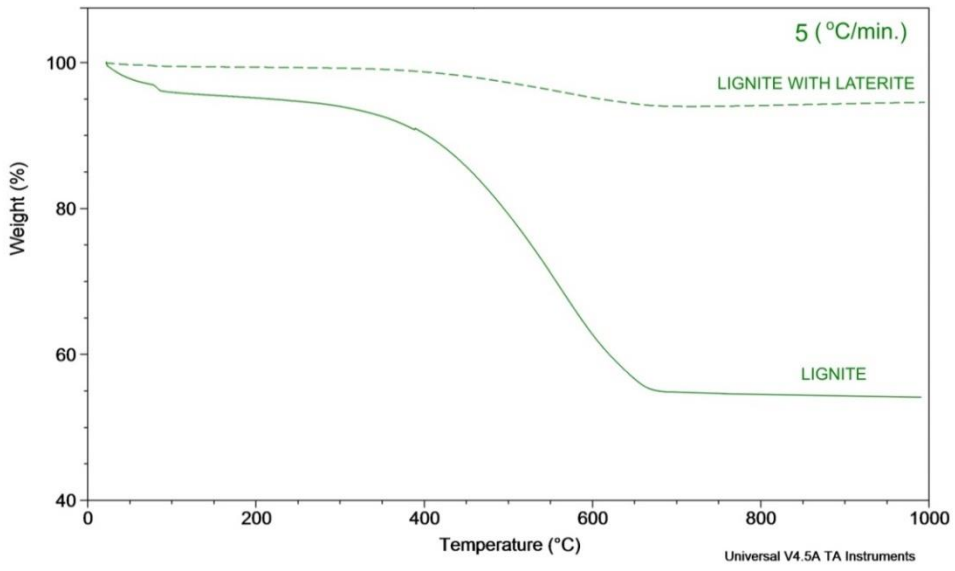

Figure 4.1 Weight loss of lignite and lignite-laterite mixture at 5 ºC/min. heating rate

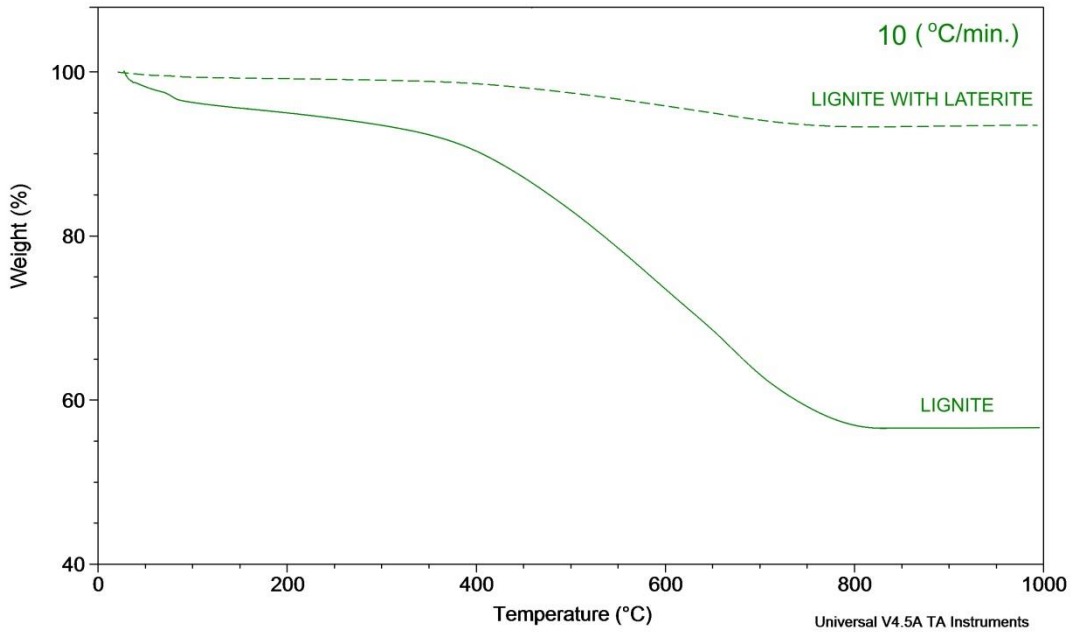

Figure 4.2 Weight loss of lignite and lignite-laterite mixture at 10 ºC/min. heating rate

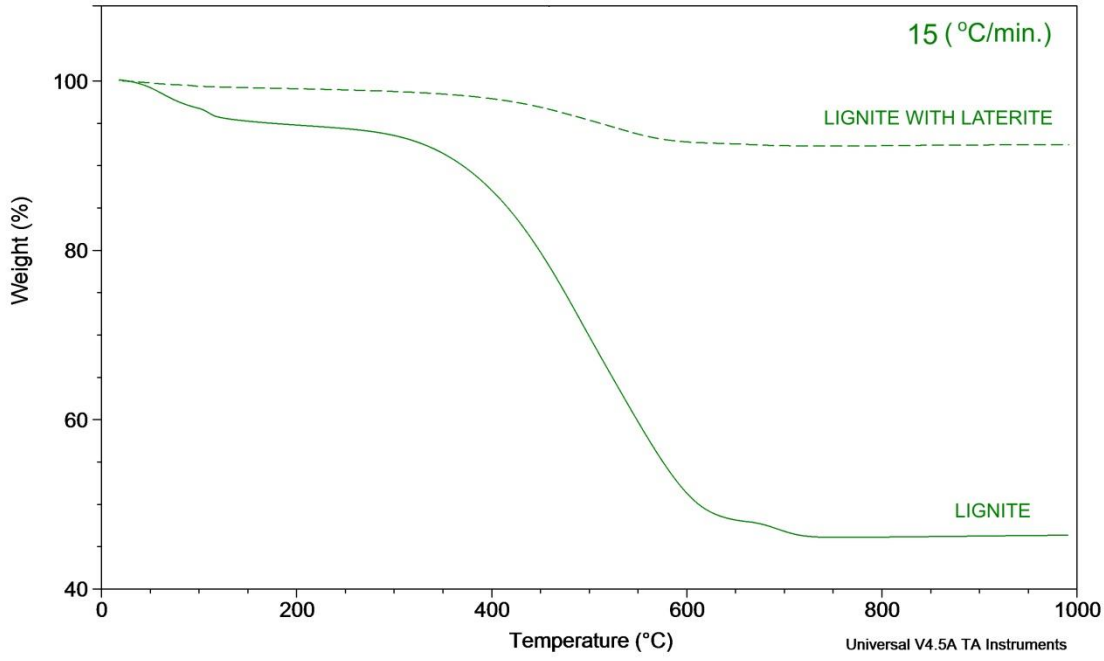

Figure 4.3 Weight loss of lignite and lignite-laterite mixture at 15 ºC/min. heating rate

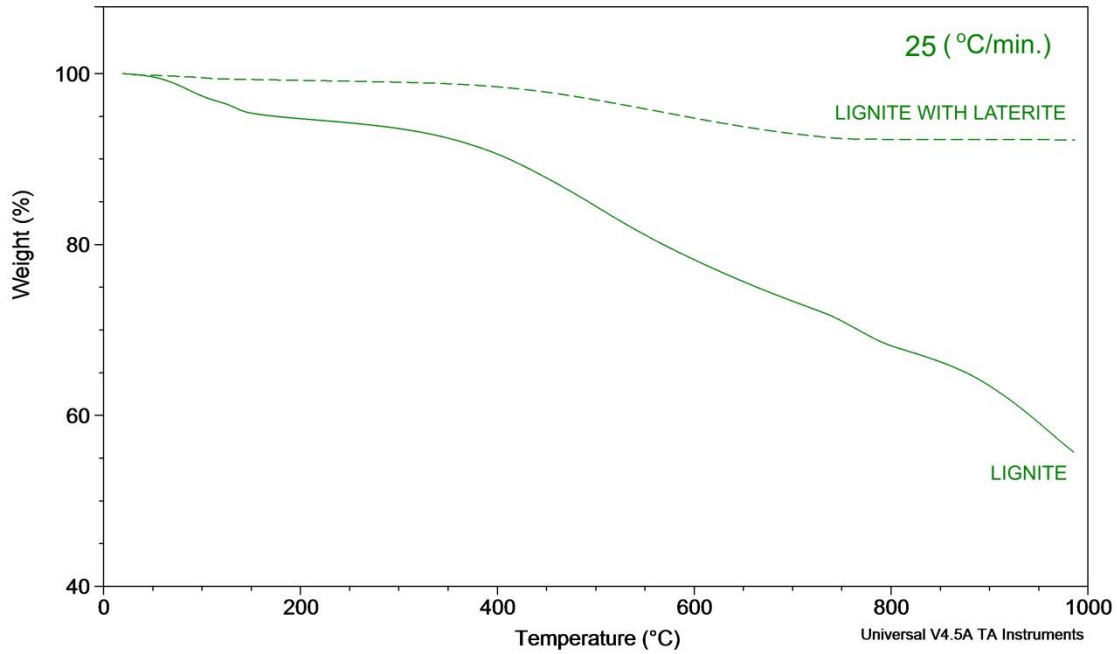

Figure 4.4 Weight loss of lignite and lignite-laterite mixture at 25 ºC/min. heating rate

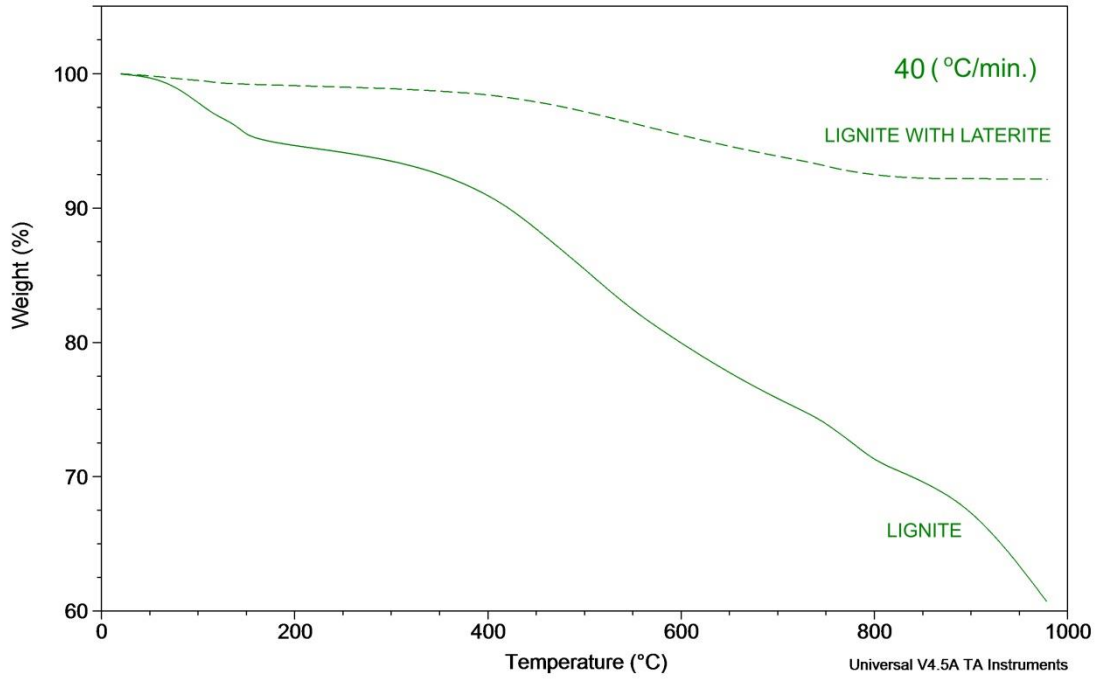

Figure 4.5 Weight loss of lignite and lignite-laterite mixture at 40 ºC/min. heating rate

4.2 Reduction Degree

The reduction degree of the calcined Gördes laterite samples by Soma lignite was calculated by the help of the TGA data according to the method explained in Section 3.3. The obtained results for various heating rates were graphed as seen in Figure 4.6.

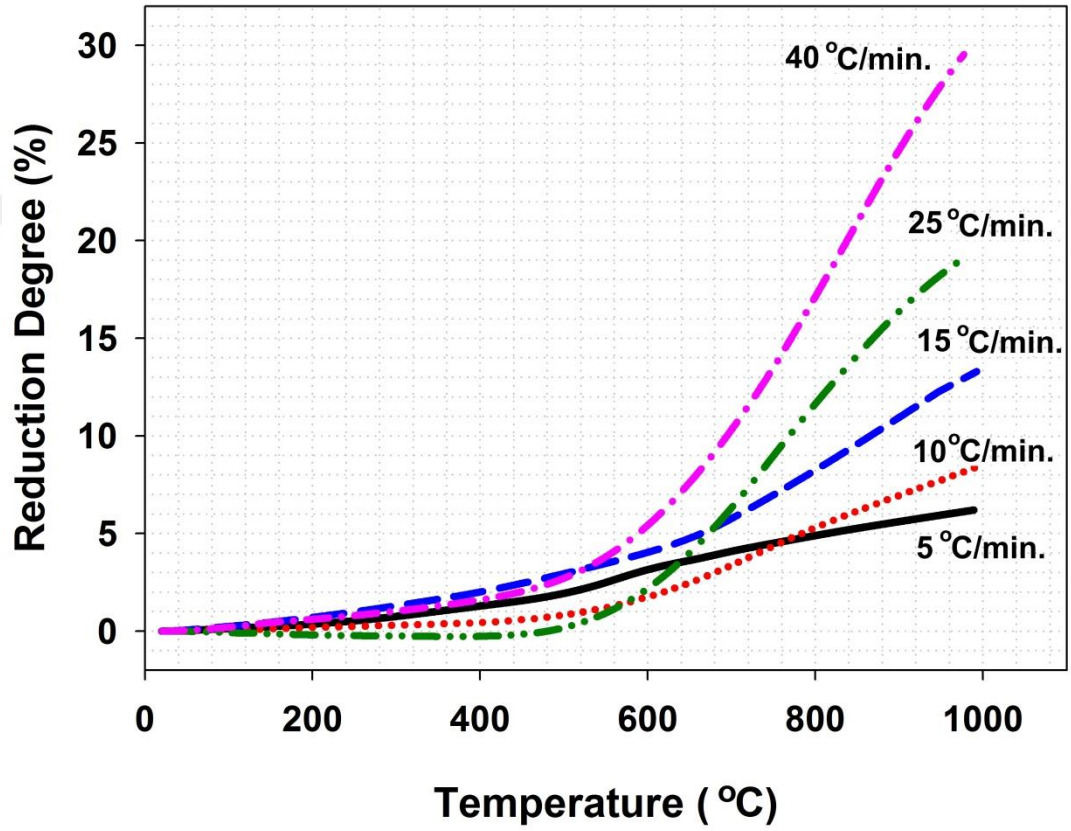

Figure 4.6 Variation of the reduction degree of the calcined laterite samples by Soma coal in TGA at various heating rates

As seen in Figure 4.6, the carbothermic reduction behavior of the laterite samples was highly sensitive to the heating rate, especially after 600 ºC, while maximum 30% reduction could be achieved at the highest heating rate most likely due to the low concentration of the lignite in the mixtures. These findings strengthen the argument that the reduction reaction occurred mostly under chemical reaction control.

4.3 Non-Isothermal Reduction Kinetics

Non-isothermal kinetic data obtained during the carbothermic reduction of calcined Gördes laterite by Soma lignite was firstly examined via various isoconversional methods such as; the differential model-free Friedman (FR) method, the integral model-free Flynn-Wall-Ozawa (FWO) method, and the integral model-free Kissinger-Akahira-Sunose (KAS) method to determine the activation energy of the process regardless of the model. The obtained graphs are given in Figure 4.7, Figure 4.8, and Figure 4.9 respectively. It should be kept in the mind that, since the abovementioned methods utilize the "conversion" instead of the "reduction degree", "α" which corresponds to one percent of the reduction degree was used for the further kinetic evaluations.

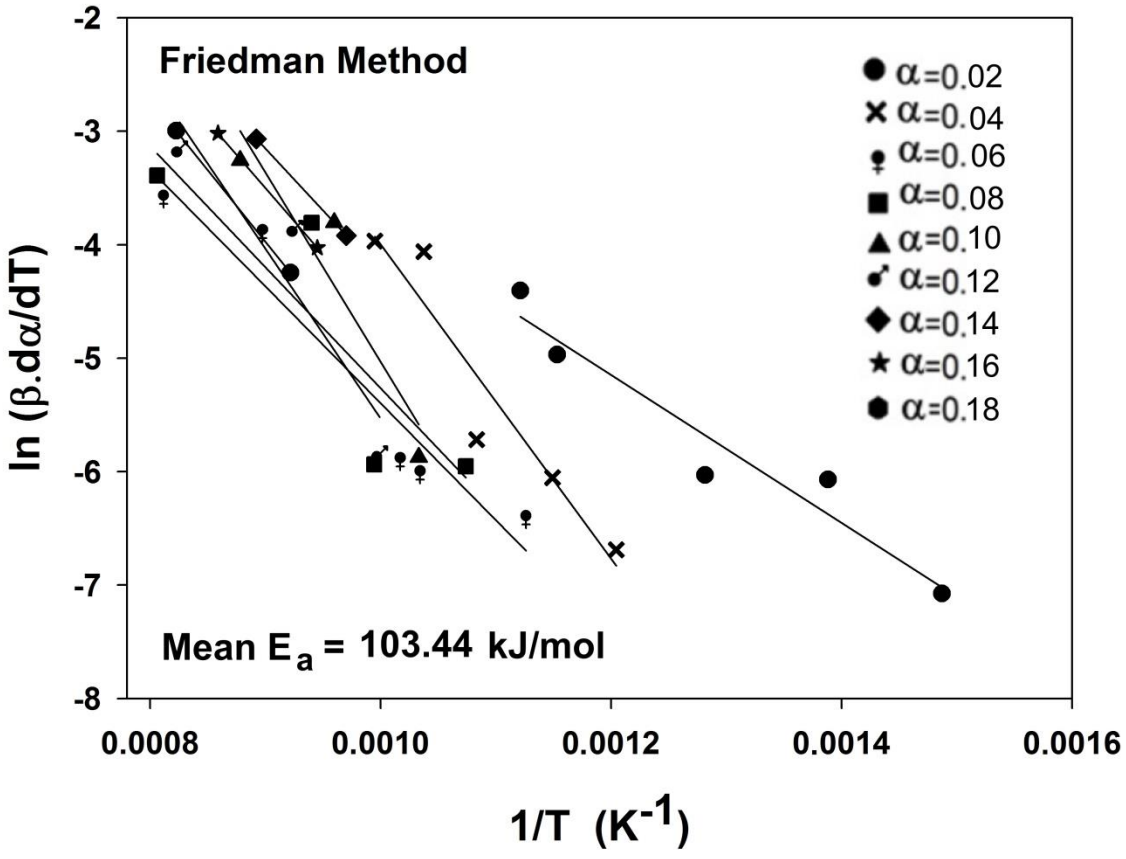

Figure 4.7 Determination of mean "E_a" for conversion levels between 0 and 0.18 using the Friedman method

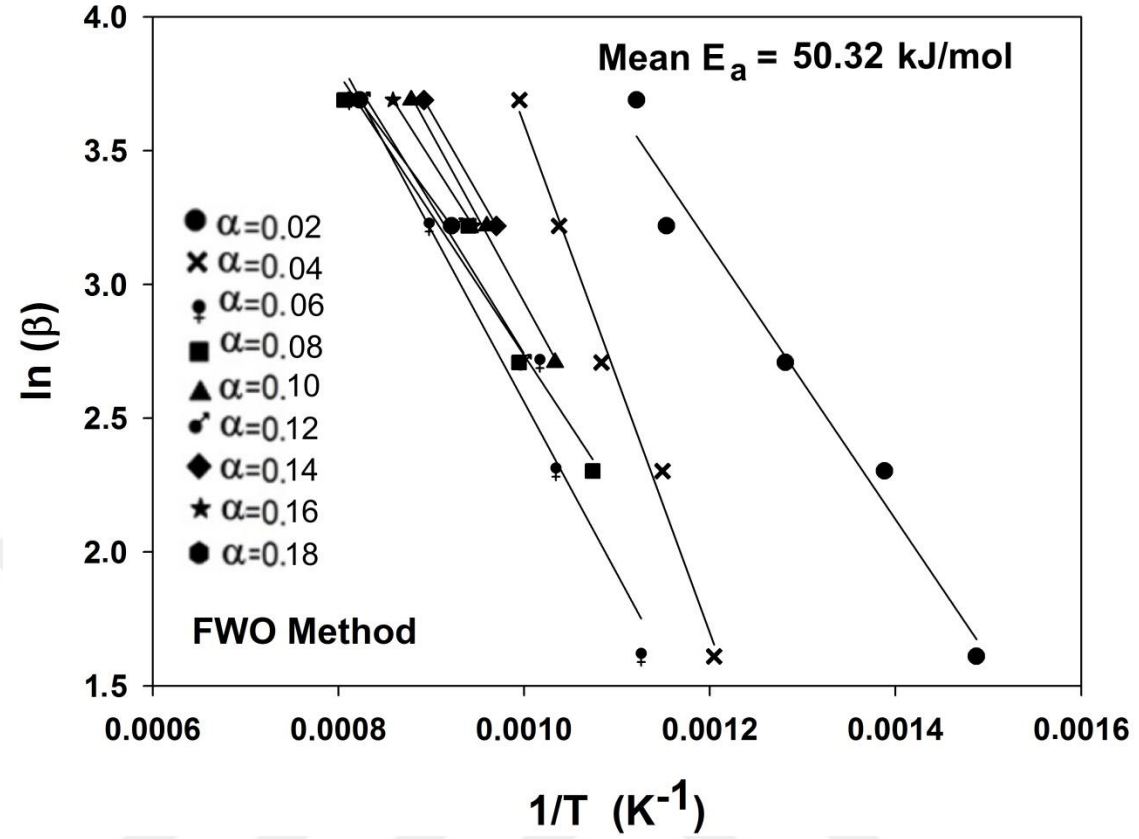

Figure 4.8 Determination of mean "E_a" for conversion levels between 0 and 0.18 using the Flynn-Wall-Ozawa (FWO) method

The mean E_a between 0 and 0.18 conversion during carbothermic reduction of calcined Gördes laterite by Soma lignite was determined as 103.44 kJ/mole, 50.32 kj/mole, and 65.68 kJ/mole via FR, FWO, and KAS methods, respectively. Two points should be emphasized based on the obtained results. First, the differential model-free Friedman (FR) method overestimated the mean E_a value (about 2 times), compared to the integral model-free Flynn-Wall-Ozawa (FWO), and Kissinger-Akahira-Sunose (KAS) methods as a common fact in the related literature.

Second, due to the low concentration of the lignite in the mixtures, the highest reduction was stricted as 30%, therefore, the mean "E_a" could be determined for a limited and low conversion range *i.e* for α values between 0 and 0.18.

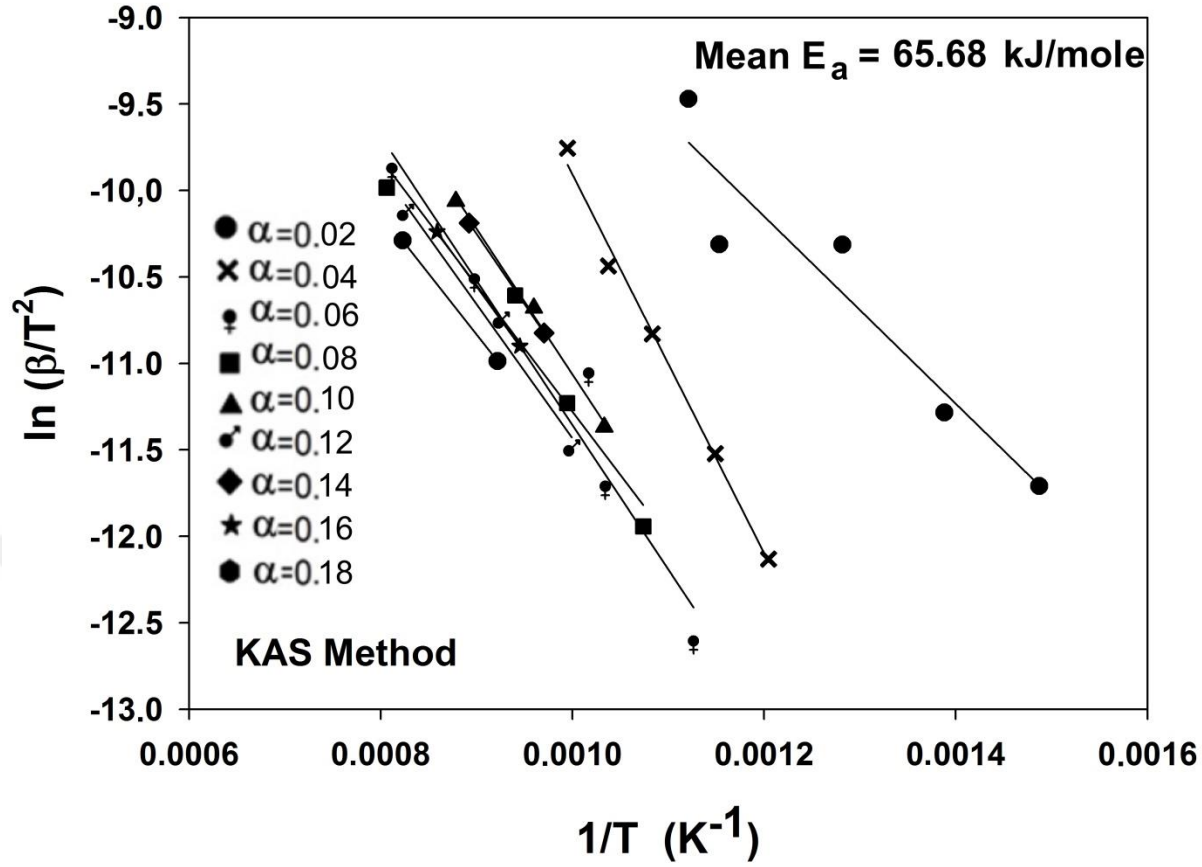

Figure 4.9 Determination of mean "E_a" for conversion levels between 0 and 0.18 using the Kissinger-Akahira-Sunose (KAS) method

After having an idea about the activation energy by the FR, FWO, and KAS methods, -albeit for a low conversion interval- full kinetic analysis performed by using the Coats-Redfern method formulated by Eq. 1.11. For that purpose, the non-isothermal "α vs t" data obtained at 40 ^{o}C/min. heating rate was converted into "$\ln[g(\alpha)/T^2]$" vs "1/T" graphs for all models given in Table 1.2. The best fitting model with the highest R^2, in other words the integral reaction model ($g(\alpha)$) of the reduction process was determined as "F0" as seen in Figure 4.10. By this way, the kinetic triplet *i.e*, the rate controlling mechanism, the mean activation energy (E_a), and the Arrhenius frequency factor (A) was determined as; phase boundary chemical reaction control, 60.01 kJ/mole, and 1.44 $l^{n-1}.mole^{1-n}.s^{-1}$, respectively for the initial stages (between 0 and 0.30 conversion) of the carbothermic reduction of calcined Gördes laterite with Soma lignite.

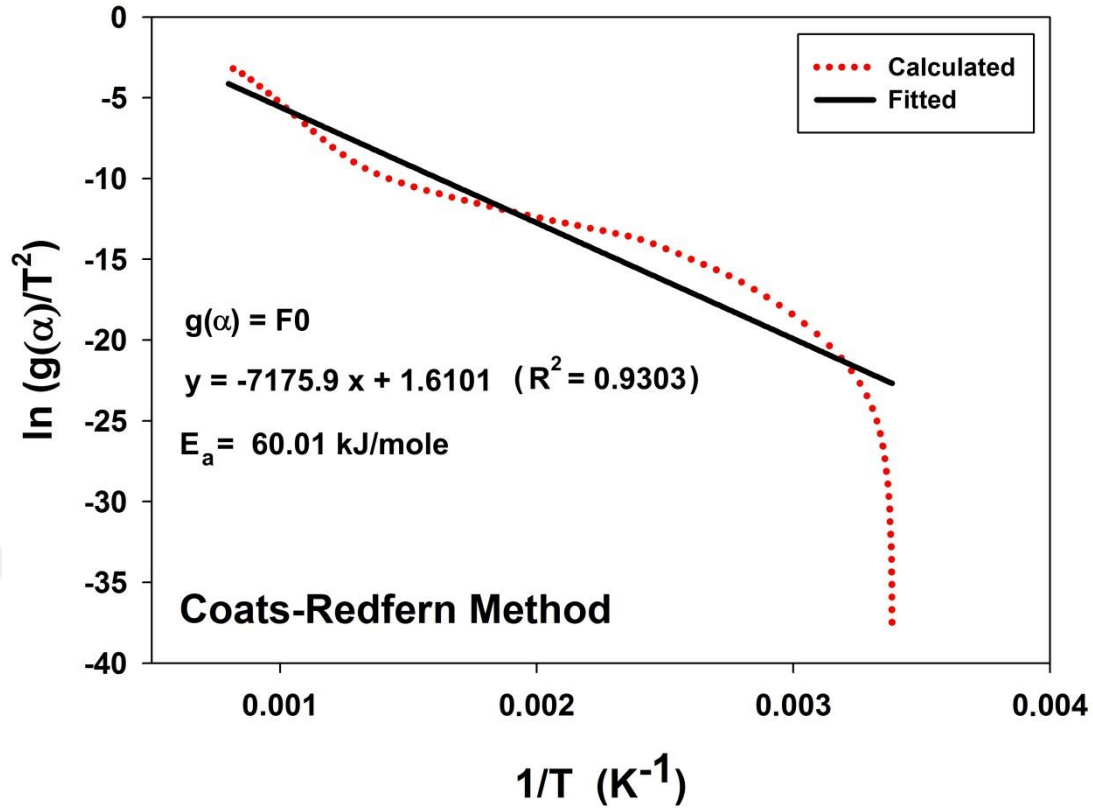

Figure 4.10 Determination of kinetic triplet using the Coats-Redfern (CR) method

5. CONCLUSIONS AND RECOMMENDATION

The main findings of this study can be summarized as follows;

1. Due to the low solid reductant concentration in laterite-lignite mixtures, the maximum reduction degree of metallic oxides in the ore stricted by approximately 30%. To enlight the full conversion mechanism of the metallic oxides in Gördes laterite into ferronickel, it is highly recommended to perform further experiments with higher lignite concentrations.

2. It was observed that as the heating rate increased, the weight loss and as well, the reduction degree of the "laterite- lignite" mixtures increased. The sensitivity of the reduction degree against the reductant concentration and the heating rate indicated that the first stages of the reduction took place under the control of the chemical reaction. In fact, it is unlikely that any product film exists that can control the rate of the process during the initial stages of reduction (between 0 and 0.3 conversions).

3. Isoconversional nonisothermal kinetic analysis of the TGA data revealed that the mean E_a between 0 and 0.18 extend during carbothermic reduction of calcined Gördes laterite by Soma lignite was as; 103.44 kJ/mole, 50.32 kj/mole, and 65.68 kJ/mole according to the FR, FWO, and KAS methods, respectively.

4. The kinetic triplet for the initial stages *i.e* 0 to 0.3 conversion levels, of the carbothermic reduction of calcined Gördes laterite with Soma lignite was identified by the model-fitting Coats-Redfern method. The phase boundary chemical reaction control characterized by "F0" integral model function was determined to be the controlling mechanism while, the mean activation energy (E_a), and the Arrhenius frequency factor (A) was calculated as 60.01 kJ/mole, and 1.44 $l^{n-1}.mole^{1-n}.s^{-1}$, respectively.

REFERENCES

Bartocci P., Tschentscher R., Stensrød R.E., Barbanera M. and Fantozzi F. 2019. Kinetic analysis of digestate slow pyrolysis with the application of the master-plots method and independent parallel reactions scheme. Molecules, 24(9):1657-1672.

Bunjaku A., Kekkonen M. and Holappa L. 2010. Phenomena in thermal treatment of lateritic nickel ores up to 1300ºC. International Ferroalloys Congress, Helsinki.

Canterford B.J.H. 1975. The treatment of nickeliferous laterites. Miner. Sci. Eng., 7 (1): 3-17.

Canterford B.J.H. and Turnbull A.G. 1980, Reduction of nickeliferous laterites: thermodynamic considerations. Proc. Aust. Inst. Min. Metall., 275:43-51.

Coats A. and Redfern J. 1963. Thermogravimetric analysis-A review. Analyst, 88 (1053): 906-924.

Conard B.R., McAneney T.B. and Sridhar R. 1978. Thermodynamics of iron-nickel alloys by mass spectrometry. Metall. Mater. Trans. B-Process Metall. Mater. Process Sci., 9: 463–468.

Dalvi A.D., Bacon W.G. and Osborne R.C. 2004. The past and the future of nickel laterites. PDAC 2004 International Convention Trade Show and Investors Exchange, Toronto.

Diaz C., Landolt C., Vahed A., Warner A. and Taylor, J. 1988. A review of nickel pyrometallurgical operations. JOM, 40(9): 28-33.

Elliott R., Rodrigues F., Pickles C. and Peacey J. 2015. A two-stage thermal upgrading process for nickeliferous limonitic laterite ores. Canadian Metallurgical Quarterly, 54(4): 395-405.

Halikia I., Skartados K. and Neou-Syngouna P. 2002 Effect of reductive roasting on smelting characteristics of Greek nickel laterites. Mineral Processing and Extractive Metallurgy, 111(3):135-142.

Fedunik-Hofman L., Bayon A., Hinkley J., Lipiński W. and Donne S.W. 2019. Friedman method kinetic analysis of CaO-based sorbent for high-temperature thermochemical energy storage. Chem. Eng. Sci., 200: 236-247.

Janković B., Adnadević B. and Mentus S. 2008. The kinetic study of temperature-programmed reduction of nickel oxide in hydrogen atmosphere. Chem. Eng. Sci., 63: 567–575.

King M. G. 2005. Nickel laterite technology—Finally a new dawn? JOM, 57(7): 35-39.

Li B., Ding Z., Wei Y., Wang H., Yang Y. and Barati M. 2018. Kinetics of reduction of lowgrade nickel laterite ore using carbon monoxide. Metall. Mater. Trans. B-Process Metall. Mater. Process Sci., 49: 3067–3073.

Lv X., Lv W., Wang L. and Qiu J. 2017. Thermal analysis kinetics of the solid-state reduction of nickel laterite ores by carbon. 8th International Symposium on High Temperature Metallurgical Processing, California.

Lv X., Lv W., You Z., Lv X. and Bai C. 2018. Non-isothermal kinetics study on carbothermic reduction of nickel laterite ore. Powder Technol., 340: 495-501.

Marzoughi O., Anthony W., Rodrigues F., Elliott R., Peacey J. and Pickles C.A. 2020. Mechanism of carbothermic reduction of a sulfur-containing nickeliferous limonitic laterite ore. Mineral Processing and Extractive Metallurgy, 129(3): 267-281.

Purwanto H., Shimada T., Takahashi R., and Yagi J. 2003. Recovery of nickel from selectively reduced laterite ore by sulphuric acid leaching. ISIJ International, 43(2): 181-186.

Rhamdhani M., Hayes P. and Jak E. 2009. Nickel laterite Part 1–microstructure and phase characterisations during reduction roasting and leaching. Mineral Processing and Extractive Metallurgy, 118(3): 129-145.

Ubando A.T., Chen W.H. and Ong H.C. 2019. Iron oxide reduction by graphite and torrefied biomass analyzed by TG-FTIR for mitigating CO_2 emissions. Energy, 180: 968-977.

Utigard T. and Bergman R.A. 1993. Gaseous reduction of laterite ores. Metall. Mater. Trans. B-Process Metall. Mater. Process Sci., 24: 271–275.

Vyazovkin S. and Wight C.A. 1999. Model-free and model-fitting approaches to kinetic analysis of isothermal and nonisothermal data. Thermochimica Acta, 340: 53-68.

Wang Z., Xie T., Ning X., Liu Y. and Wang, J. 2019. Thermal degradation kinetics study of polyvinyl chloride (PVC) sheath for new and aged cables. Waste Manag., 99: 146-153.

Warner A.E.M., Díaz C.M., Dalvi A.D., Mackey P.J., Tarasov A.V. and Jones R.T. 2006. JOM world nonferrous smelter survey Part IV: Nickel: Sulfide. JOM, 59(4), 58–72.

Zhang Y., Cui K., Wang J., Wang X., Qie J.,Xu Q. and Qi Y. 2020. Effects of direct reduction process on the microstructure and reduction characteristics of carbon-bearing nickel laterite ore pellets. Powder Technol., 376: 496-506.

Zhua D., Pan L., Guo Z., Pan, J. and Zhang F. 2012. Utilization of limonitic nickel laterite to produce ferronickel concentrate by the selective reduction-magnetic separation process. Adv. Powder Technol., 30: 451–460.

CURRICULUM VITAE

Personal Information

Name and Surname : Ahmed Mures Mohammed MOHAMMED

Education

MSc	Çankırı Karatekin University Graduate School of Natural and Applied Sciences Department of Chemical Engineering	2020-2023
Undergraduate	Tikrit University Faculty of Engineering Department of Chemical Engineering	1997-2002

Work Experience

Year	**Institution**	**Position**
2005-Present	North Refinery Co.	Chief Engineer